Analysis and simulation of a dynamic reconfiguration algorithm for a photovoltaic array

L. M. Martínez-Rugerio * **J. F. Guerrero-Castellanos** *

* *Benemérita Universidad Autónoma de Puebla, Facultad de Ciencias de la Electrónica, Puebla, México (e-mail: liliana.martinezru@alumno.buap.mx, fermi.guerrero@correo.buap.mx).*

Abstract: This article presents the development of a simulator and an in-depth analysis of two dynamic reconfiguration algorithms for photovoltaic arrays. The analyzed dynamic reconfiguration algorithms (ERA and SRA) are based on the concept of "irradiance equalization", which seeks to reduce the partial shading effect's losses. Both algorithms work in a Total-Cross-Tied (TCT) architecture and differ by the strategy used. The obtained results are analyzed, and a comparison with traditional schema is carried out to assess its effectiveness. Some recommendations for real-time implementation are outlined.

Keywords: Partial Shading, Irradiance Equalization Index, Dynamic Photovoltaic Arrays (DPVAs), Sorting Reconfiguration Algorithm (SRA), Exhaustive Evaluation Reconfiguration Algorithm (ERA).

1. INTRODUCTION

Nowadays, the world energy system is based mainly on fossil fuels that generate emissions of polluting gases and consume many other resources, such as water. Due to its negative impact, it is necessary to promote research and development of renewable energies as an alternative to generate energy in a cleaner and more efficient way.

In the specific case of solar energy, México is one of the five countries with the greatest potential in the world. The average solar energy the country receives is 5kWh per square meter per day (Klapp et al. (2007)).

The concept of "solar energy" refers mainly to the use of solar radiation for the generation of useful energy. The photoelectric effect is the principle of operation of solar cells, devices based on the p-n junction, whose electrons are displaced to the conduction band due to the energy contribution of incident photons. The current of a solar cell is a balance between the photocurrent and the dark current, which depends on the voltage applied to the terminals of the device. When the voltage applied is zero (short-circuited cell) the current is due exclusively to the photocurrent. The value of the current remains almost constant until it is close to the voltage value at which the diode starts to conduct. From this point, the current decreases abruptly until it reaches a zero value (open circuit cell) at the point where the photocurrent and dark current are compensated (Lamigueiro (2013)). The two end points of short circuit and open circuit are defined by two parameters, the short circuit current, I_{sc}, and the open circuit voltage, V_{oc}.

A photovoltaic generator is made up of $N_p \cdot N_s$ modules, where N_p is the number of rows and N_s is the number of modules connected in each series. The total generator current is calculated as $I_g = N_p \cdot I_m$, on the other hand, the total generator voltage is calculated as $V_g = N_s \cdot V_m$ (Lamigueiro (2013)).

Currently, the installation of photovoltaic arrays in urban areas is increasing and the partial shading is the major cause for mismatch losses which can reduce considerably the energy yield of photovoltaic systems (Belhachat and Larbes (2015)). As the sun traverses the sky, the presence of buildings and other objects will cast "block" shadows that move as the sun orientation changes (Storey et al. (2014)). Therefore, estimation of the power yield under different environmental conditions, finding methods to overcome the negative effects mentioned and finally improving the efficiency of the PV generation systems has been considered by many researchers during the recent years (Jazayeri et al. (2014)).

The dynamic reconfiguration algorithms are based on the idea that losses related to the shading effect can be reduced through the reorganization of the photovoltaic modules. The studied algorithms work with a Total-Cross-Tied (TCT) architecture and are classified as different types of control algorithms. The first is called an Exhaustive Evaluation Reconfiguration Algorithm (ERA) ,and the second as a Sorting Reconfiguration Algorithm

(SRA). The main objective of the ERA algorithm is to reduce the calculation time by decreasing the width of the search space, while the SRA algorithm the photovoltaic elements are organized on the basis of the irradiance level each one of them is receiving.

However, the reported algorithms have not been simulated in-depth by analyzing their response to different partial shading scenarios, which devalues their importance, in addition to having uncertainty in the reliability of their application in real-time.

This paper aims to show the development of a simulator of photovoltaics arrays in MATLAB/Simulink. With this simulator, the photovoltaics arrays' configuration can be changed dynamically. The reconfiguration is carried out according to two algorithms [Velasco-Quesada et al. (2009)],[Storey et al. (2013)]. The electrical characteristics of the simulated systems are the ones of the FCE-BUAP's Photovoltaic system. A comparison between the two mentioned algorithms and the conventional configuration is shown.

The rest of the paper is organized as follows: Section II is devoted to present two dynamic reconfiguration algorithms for photovoltaic arrays, the development of simulations is given in Section III, Section IV analyses the results, the guidelines for real-time implementation are proposed in Section V and finally the conclusions are expressed in Section VI.

2. DYNAMIC RECONFIGURATION ALGORITHMS

2.1 Exhaustive Evaluation Reconfiguration Algorithm (ERA)

(Velasco-Quesada et al. (2009)) propose a dynamic reconfiguration strategy for a grid-connected photovoltaic system. The proposed ERA strategy is carried out through the implementation and control of a switching matrix, which allows the electrical reconnection of the photovoltaic modules.

The steps in the reconfiguration strategy are listed below:

(1) Setting initial conditions
The algorithm assumes that the irradiance value of each module is known and is noted as G_{ij}, where $i = 1, ..., m$ and $j = 1, ..., n$ stand for the row and the column, respectively, where the module is initially located. Once the values of m and n are known, and assuming that all the values of the irradiance G_{ij} are different, the algorithm computes all the configurations of interest defined in (1). Each of these configurations is identified as A_k, where $k = 1, 2, ..., K$.

$$A_k = \frac{(m \cdot n)!}{m! \cdot (n!)^m} \quad (1)$$

(2) Computation of average irradiance present at each row
For each of the configurations of interest A_k, the algorithm computes the average irradiance on the n parallel-connected modules of each row defined in (2).

$$G_{ik} = \frac{\sum_{j=1}^{n} G_{ijk}}{n} \quad i = 1, 2, ..., m \quad k = 1, 2, ..., K, (2)$$

(3) Computation of "Irradiance Equalization Index"
This index is defined to quantify how different are the average irradiances present at each row and consequently what is the degree of current limitation of the configuration. A simple way to define the irradiance equalization index of the configuration A_k referred as $M_{IE}(A_k)$ is defined in (3).

$$M_{IE}(A_k) = max\,[G_{1k}, G_{2k}, ..., G_{mk}] - min \quad (3)$$
$$[G_{1k}, G_{2k}, ..., G_{mk}] \quad for \quad k = 1, ..., K$$

(4) Computation of number of photovoltaic module relocations
This index evaluates the number of modules to be relocated when the photovoltaic generator is reconfigured from the current configuration.

(5) Reconfiguration decision making
The decision making is structured in three hierarchical levels:
   (a) The first level of decision disables the reconfiguration of the switching matrix if the optimum configuration is the same that the initial one.
   (b) The second level asks for a possible module failure.
   (c) The third decision level enables the reconfiguration of the switching matrix only if the optimum configuration is stable (i.e., if it remains the same) during a certain amount of time.

2.2 Sorting Reconfiguration Algorithm (SRA)

(Storey et al. (2013)) propose an improved strategy for the optimization of dynamic photovoltaic arrays (DPVAs) utilizing the "Irradiance Equalization" reconfiguration strategy. This array of modules can be configured in any form in terms of rows and columns.

The steps in the reconfiguration strategy are listed below:

(1) Based on the irradiance data of each module, the columns are sorted in descending order.
(2) The even columns in the array are ordered from lowest to highest.
(3) The columns of the array are joined in pairs and the irradiances are averaged in rows.
(4) Odd module joints are ordered based on the average by rows from highest to lowest and even module joints are ordered based on the average by rows from lowest to highest.

The algorithm requires the number of columns to be of power two; otherwise, an extra column of zeros can be added.

3. SIMULATION OF ALGORITHMS

The simulations of both algorithms in MATLAB/Simulink represent the FCE-BUAP's photovoltaic system as a 3x4 TCT array. These simulations are intended to evaluate the performance of reconfigurable arrays under three proposed shading scenarios. Table 1 shows the irradiance values of each photovoltaic module in its corresponding position.

Table 1. Shading scenarios proposed

FIRST SCENARIO			
1000	900	900	900
1000	950	900	900
1000	150	100	100
SECOND SCENARIO			
1000	900	800	800
500	450	450	430
210	280	250	210
THIRD SCENARIO			
1000	1000	500	450
1000	950	500	550
550	700	200	150

The writing of the dynamic reconfiguration algorithms is done in the editor of the "MATLAB function" block in Simulink, where the system inputs and outputs are specified. In this case, the response of the dynamic reconfiguration of the photovoltaic systems depends entirely on the input (irradiance of each module), and in both cases, the output or response of the system is reflected in a switching matrix. The switching matrix is composed of a set of switches, which turn on or off according to the described algorithm, in order to achieve a certain reconfiguration for the photovoltaic system.

According to the number of simulated modules and the characteristics of the switches available in Simulink, 72 Single Pole Single Throw (SPST) switches are used; however, we would only need 24 Single Pole Triple Trow (SPTT) switches (not available in Simulink). This factor does not represent a limitation, it only makes the visualization of the simulation more complex.

To understand the use of each switch, consider that per PV module three are occupied for the positive connection and three for the negative connection, the turning on or off of each one depends on the binary value 1-on or 0-off that is assigned to each one within the development of the algorithm. In general, table 2 shows the relationship between each switch and each photovoltaic module (PVM), indicating which switches, when turned on, allow the modules to be in their original position and which allow each module to be relocated to other rows (R).

Fig. 1 shows the visual environment of the simulations performed in Simulink, such environment is the same for both algorithms. The red oval indicates the inputs (irradiances of the photovoltaic array) of the "MATLAB Function" block, the blue represents the switching matrix (i.e. 72 switches), the brown one indicates the first Single Pole Single Throw switch (S1) in the simulation, the green one indicates a photovoltaic module, the orange one indicates an irradiance constant, the pink one shows the I-V and P-V curve plotters of the array, and finally the yellow one shows the results of the possible configurations and the configurations of interest.

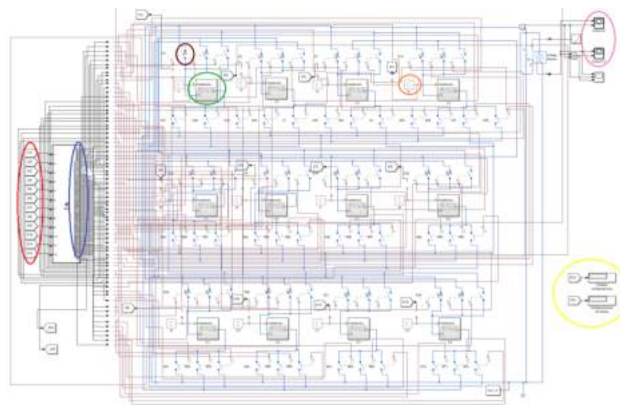

Fig. 1. Visual environment in MATLAB/Simulink

Table 2. Switches corresponding to each PVM

		R1 (+)	R2 (+)	R3 (+)	R1 (-)	R2 (-)	R3 (-)
R1	PVM 1	S1	S2	S3	S37	S38	S39
	PVM 2	S4	S5	S6	S40	S41	S42
	PVM 3	S7	S8	S9	S43	S44	S45
	PVM 4	S10	S11	S12	S46	S47	S48
		R2 (+)	R1 (+)	R3 (+)	R2 (-)	R1 (-)	R3 (-)
R2	PVM 5	S13	S14	S15	S49	S50	S51
	PVM 6	S16	S17	S18	S52	S53	S54
	PVM 7	S19	S20	S21	S55	S56	S57
	PVM 8	S22	S23	S24	S58	S59	S60
		R3 (+)	R1 (+)	R2 (+)	R3 (-)	R1 (-)	R2 (-)
R3	PVM 9	S25	S26	S27	S61	S62	S63
	PVM 10	S28	S29	S30	S64	S65	S66
	PVM 11	S31	S32	S33	S67	S68	S69
	PVM 12	S34	S35	S36	S70	S71	S72

For both algorithms, inside the "MATLAB Function" block are indicated as outputs: the variables "pc" and "ci", which represent the possible configurations and the configurations of interest, respectively, and each switch with the nomenclature $S(i)$, where $i = 1, ..., 72$. Immediately, the function inputs (twelve variables representing the irradiances of the modules) are indicated as $I(n)$, where $n = 1, ..., 12$.

Then, the initial configuration of the photovoltaic array with the TCT architecture is indicated by writing the binary values corresponding to each switch (according to table 1). After the algorithms know the initial configuration of the array and the irradiance of each module (values previously entered from Simulink), they can start.

The writing of the algorithms is supported by the use of conditional sentences (if and elseif) that allows them to carry out an action if a certain condition is met and also if it is not. The first sentence "if" is responsible for comparing the irradiances between them and, if they are equal, the binary values of each switch remain the same as in the initial configuration and simply ends the execution of the algorithm. The scenarios proposed in table 1 suggest shading conditions, so in this case the algorithms will always discard the content of the first conditional sentence and reconfigure the array according to their methodology.

4. RESULTS

The evaluation of the dynamic reconfiguration algorithms is based on the comparison of the obtained I-V and P-V characteristic curves and on the evaluation of the capacity of each algorithm to decrease the "Irradiance Equalization Index" in each shading scenario (table 1).

4.1 First proposed shading scenario

The first scenario suggests a significant case of shading on most of the PV modules in the last row. Fig. 2 shows the characteristic curves obtained, where it can be seen that the array reconfigured with the SRA algorithm shows the best results, increasing the short circuit current 114.81% with respect to the fixed connection system and 31.81% compared to the system reconfigured with the ERA algorithm. In contrast, the array reconfigured with the ERA algorithm increased the short circuit current by 62.96% compared to the fixed connection system. The improved power response of the reconfigurable arrays is evident in the P-V characteristic curves.

The ERA algorithm relocated to modules 5 and 10, while the SRA algorithm reconfigured to modules 1, 4, 5, 8, 9 and 12.

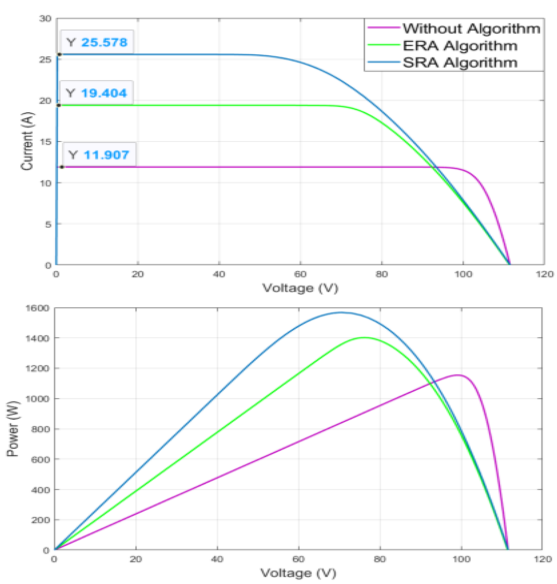

Fig. 2. I-V and P-V characteristic curves obtained

On the other hand, table 3 shows the calculations of the average irradiance per row (AIR) and the absolute difference between the overall average of irradiance and AIR for a conventional photovoltaic array (fixed-connection) under conditions of the first proposed shading scenario. The objective of the analysis is to know the overall average of distance between irradiances per row, i.e. the irradiance equalization index.

Tables 4 and 5 allow us to analyse that ERA algorithm reduced the equalization index by 51.58% and the SRA algorithm by 97.89%.

Table 3. Irradiance equalization analysis for a fixed-connection array

AIR	Overall average-AIR
925	191.66
937.5	204.16
937.5	395.83
Average	**Equalization index**
733.33	**263.88**

Table 4. Irradiance equalization analysis for a reconfigured array with the ERA algorithm

AIR	Overall average-AIR
925	191.66
725	8.33
550	183.33
Average	**Equalization index**
733.33	**127.77**

Table 5. Irradiance equalization analysis for a reconfigured array with the SRA algorithm

AIR	Overall average-AIR
737.5	4.16
725	8.33
737.5	4.16
Average	**Equalization index**
733.33	**5.5**

4.2 Second proposed shading scenario

The second scenario suggests a significant case of shading especially for the modules in rows 2 and 3. Fig. 3 shows the characteristic curves obtained, where it can be seen that the array reconfigured with the SRA algorithm shows the best results, increasing the short circuit current 116.84% with respect to the fixed connection system and 21.17% compared to the system reconfigured with the ERA algorithm. In contrast, the array reconfigured with the ERA algorithm increased the short circuit current by 78.94% compared to the fixed connection system. The P-V characteristic curves show a better response in the power output by the reconfigurable arrays.

The ERA algorithm relocated to modules 1 and 11, while the SRA algorithm reconfigured to modules 1, 3, 5, 6, 8, 9, 10, 11 and 12.

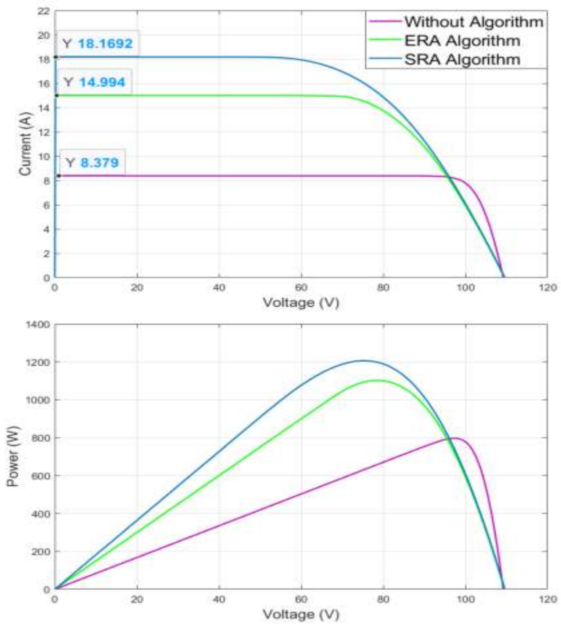

Fig. 3. I-V and P-V characteristic curves obtained

Table 6 shows the irradiance equalization analysis for a fixed-connected photovoltaic array under the proposed scenario.

Tables 7 and 8 show that with the application of the ERA algorithm, the irradiance equalization index was reduced by 53.31% and with the SRA algorithm by approximately 97.39%.

Table 6. Irradiance equalization analysis for a fixed-connection array

AIR	Overall average-AIR
875	351.66
457.5	65.83
237.5	285.83
Average	**Equalization index**
523.33	**234.44**

Table 7. Irradiance equalization analysis for a reconfigured array with the ERA algorithm

AIR	Overall average-AIR
687.5	164.17
457.5	65.83
425	98.33
Average	**Equalization index**
523.33	**109.44**

Table 8. Irradiance equalization analysis for a reconfigured array with the SRA algorithm

AIR	Overall average-AIR
532.5	9.16
522.5	0.83
515	8.33
Average	**Equalization index**
523.33	**6.11**

4.3 Third proposed shading scenario

The third scenario presents a case of shading where all the rows of the array are affected. Fig. 4 shows the characteristic curves obtained, where it can be seen that the array reconfigured with the SRA algorithm shows the best results, increasing the short circuit current 50% with respect to the fixed connection system and 17.07% compared to the system reconfigured with the ERA algorithm. In contrast, the array reconfigured with the ERA algorithm increased the short circuit current by 28.12% compared to the fixed connection system. The P-V curves show a better response in the power output by the array reconfigured with the SRA algorithm.

The ERA algorithm relocated to modules 5 and 9, while the SRA algorithm reconfigured to modules 1, 4, 9 and 12.

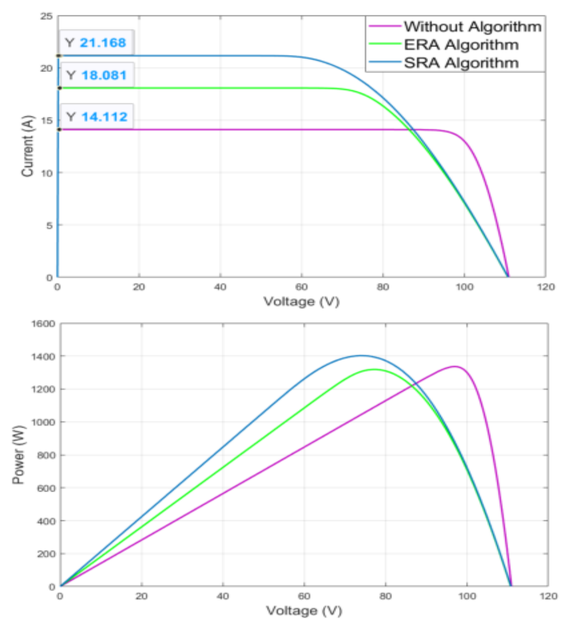

Fig. 4. I-V and P-V characteristic curves obtained

Table 9 shows the irradiance equalization analysis for a fixed-connected photovoltaic array under the proposed scenario.

Tables 10 and 11 show that with the application of the ERA algorithm, the irradiance equalization index was reduced by 49.09% and with the SRA algorithm by approximately 85.45%.

Table 9. Irradiance equalization analysis for a fixed-connection array

AIR	Overall average-AIR
737.5	108.33
750	120.83
400	229.16
Average	**Equalization index**
629.16	**152.77**

Table 10. Irradiance equalization analysis for a reconfigured array with the ERA algorithm

AIR	Overall average-AIR
737.5	108.33
637.5	8.33
512.5	116.66
Average	**Equalization index**
629.16	**77.77**

Table 11. Irradiance equalization analysis for a reconfigured array with the SRA algorithm

AIR	Overall average-AIR
662.5	33.33
600	29.16
625	4.16
Average	**Equalization index**
629.16	**22.22**

5. GUIDELINES FOR REAL-TIME IMPLEMENTATION

The indispensable guidelines for the real-time physical application of dynamic reconfiguration algorithms have electrical elements according to the dimension of the working scale.

(Ye Zhao et al. (2012)) mention the devices used for a small-scale prototype of a reconfigurable photovoltaic array. The elements mentioned are: 4 photovoltaic units (UNI-PAC15 by UNI-SOLAR), a switching matrix (9 solid-state relays ASSR-1611), a blocking diode, data logger, a microcontroller (Explorer 16 by Microchip) and the batteries (HR-3UTGA by SANYO and LC-R121R3P by Panasonic).

The structure required for the large-scale application of the algorithms as in the case of the simulated photovoltaic system (12 Sunmodule SW 265 mono photovoltaic modules), the capacity of the elements changes. The elements that stand out are the following: a switching matrix (12 SPDT relays 450 SERIES HEAVY DUTY POWER RELAY by Struthers-dunn and 12 SPST relays Power PCB Relay T9V Solar by TE Connectivity), measurement and data logging (I-V400W by HTANALYSIS) and an irradiance sensor (HT304N by HTANALYSIS).

We can observe that the general idea of operation is the same for both scales of work, we need to monitor and acquire the irradiance data of the photovoltaic system to be analyzed in a PC by the reconfiguration algorithm used and represent its response to a switching matrix.

6. CONCLUSIONS

The development of dynamic reconfiguration algorithms represents an improvement opportunity for photovoltaic installations to solve the shading effect that often decreases the performance of the previously designed system. By means of the simulations carried out, it was possible to deepen in the viability of these algorithms for different partial shading scenarios, as well as to make the comparison.

Both reconfiguration algorithms are able to improve the response of the photovoltaic system compared to the system with fixed TCT architecture; however, the SRA algorithm stood out in a higher proportion. Through the analysis of the irradiance equalization index in each proposed shading scenario, it was possible to confirm that the reduction of the index corresponds to the improvement in the response of the system, adapting to the initial irradiance conditions. The improvement in the response of a reconfigurable PV array is proportional to the complexity of the control algorithm it employs.

It is convenient as future work to consider the physical implementation to create a broader perspective. In a physical implementation it would be expected that the energy recovered would be enough to make it viable. The lifetime of the photovoltaic modules allows for a wide range of time to recover the investment, if the physical implementation is to be carried out; however, an economic study is necessary.

REFERENCES

Belhachat, F. and Larbes, C. (2015). Modeling, analysis and comparison of solar photovoltaic array configurations under partial shading conditions. *Solar Energy*, 120, 399–418. doi: https://doi.org/10.1016/j.solener.2015.07.039.

Jazayeri, M., Uysal, S., and Jazayeri, K. (2014). A comparative study on different photovoltaic array topologies under partial shading conditions. In *2014 IEEE PES T D Conference and Exposition*, 1–5. doi: 10.1109/TDC.2014.6863384.

Klapp, J., Cota, J.L.C., and Alcalá, J.F.C. (2007). Towards a cleaner planet: energy for the future. *Springer Science Business Media*.

Lamigueiro, O.P. (2013). Energía solar fotovoltaica. *Creative Commons ebook*.

Storey, J., Wilson, P.R., and Bagnall, D. (2014). The optimized-string dynamic photovoltaic array. *IEEE Transactions on Power Electronics*, 29(4), 1768–1776. doi:10.1109/TPEL.2013.2265497.

Storey, J.P., Wilson, P.R., and Bagnall, D. (2013). Improved optimization strategy for irradiance equalization in dynamic photovoltaic arrays. *IEEE Transactions on Power Electronics*, 28(6), 2946–2956. doi: 10.1109/TPEL.2012.2221481.

Velasco-Quesada, G., Guinjoan-Gispert, F., Pique-Lopez, R., Roman-Lumbreras, M., and Conesa-Roca, A. (2009). Electrical pv array reconfiguration strategy for energy extraction improvement in grid-connected pv systems. *IEEE Transactions on Industrial Electronics*, 56(11), 4319–4331. doi:10.1109/TIE.2009.2024664.

Ye Zhao, Yang, L., and Lehman, B. (2012). Reconfigurable solar photovoltaic battery charger using a switch matrix. In *Intelec 2012*, 1–7. doi: 10.1109/INTLEC.2012.6374465.

